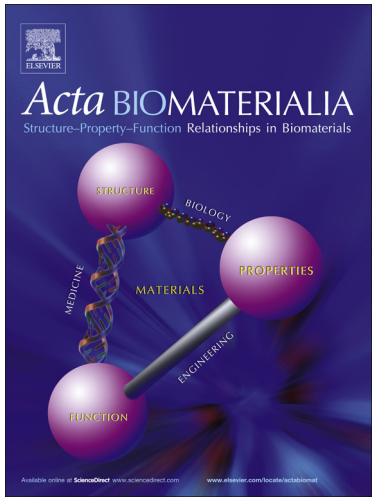

Coating of Quantum Dots strongly defines their effect on lysosomal health and autophagy

Karen Peynshaert, Stefaan J. Soenen, Bella B. Manshian, Shareen H. Doak, Kevin Braeckmans, Stefaan C. De Smedt, Katrien Remaut

PII: S1742-7061(16)30549-9
DOI: http://dx.doi.org/10.1016/j.actbio.2016.10.022
Reference: ACTBIO 4488

To appear in: *Acta Biomaterialia*

Received Date: 14 June 2016
Revised Date: 24 September 2016
Accepted Date: 15 October 2016

Please cite this article as: Peynshaert, K., Soenen, S.J., Manshian, B.B., Doak, S.H., Braeckmans, K., De Smedt, S.C., Remaut, K., Coating of Quantum Dots strongly defines their effect on lysosomal health and autophagy, *Acta Biomaterialia* (2016), doi: http://dx.doi.org/10.1016/j.actbio.2016.10.022

Coating of Quantum Dots strongly defines their effect on lysosomal health and autophagy

Karen Peynshaert[a,b], Stefaan J. Soenen[c], Bella B. Manshian[c], Shareen H. Doak[e], Kevin Braeckmans[a,d], Stefaan C. De Smedt[a,b,*], Katrien Remaut.[a,b]

[a]Lab of General Biochemistry and Physical Pharmacy, Faculty of Pharmaceutical Sciences, Ghent University, Ottergemsesteenweg 460, B9000 Ghent, Belgium.

[b]Ghent Research Group on Nanomedicines, Ghent University, Ottergemsesteenweg 460, B9000 Ghent, Belgium.

[c]Biomedical MRI Unit/MoSAIC, Department of Imaging and Pathology, Catholic University of Leuven, Faculty of Medicine, UZ Herestraat 49 Box 7003, B3000- Leuven

[d]Centre for Nano- and Biophotonics, Ghent University, B9000 Ghent, Belgium.

[e] Institute of Life Science, College of Medicine, Swansea University, Singleton Park, Swansea, SA2 8PP Wales

*Address correspondence to: Stefaan De Smedt, Ghent Research Group on Nanomedicines, Ghent University, Ottergemsesteenweg 460, B9000 Ghent, Belgium. Tel: 0032 9 264 8076 Fax: 0032 9 2648189 E-mail: Stefaan.Desmedt@ugent.be

Keywords: Quantum Dot; biocompatibility; lysosome; autophagy

Table of contents

1. ABSTRACT

In the last decade the interest in autophagy got an incredible boost and the phenomenon quickly turned into an extensive research field. Interestingly, dysfunction of this cytoplasmic clearance system has been proposed to lie at the root of multiple diseases including cancer. We therefore consider it crucial from a toxicological point of view to investigate if nanomaterials that are developed for biomedical applications interfere with this cellular process. Here, we study the highly promising 'gradient alloyed' quantum dots (QDs) that differ from conventional ones by their gradient core composition which allows for better fluorescent properties. We carefully examined the toxicity of two identical gradient alloyed QDs, differing only in their surface coatings, namely 3-mercaptopropionic (MPA) acid and polyethylene glycol (PEG). Next to more conventional toxicological endpoints like cytotoxicity and oxidative stress, we examined the influence of these QDs on the autophagy pathway. Our study shows that the cellular effects induced by QDs on HeLa cells were strongly dictated by the surface coat of the otherwise identical particles. MPA-coated QDs proved to be highly biocompatible as a result of lysosomal activation and ROS reduction, two cellular responses that help the cell to cope with nanomaterial-induced stress. In contrast, PEGylated QDs were significantly more toxic due to increased ROS production and lysosomal impairment. This impairment next results in autophagy dysfunction which likely adds to their toxic effects. Taken together, our study shows that coating QDs with MPA is a better strategy than PEGylation for long term cell tracking with minimal cytotoxicity.

2. INTRODUCTION

Nanotechnology is a rapidly evolving field with a growing potential for a wide range of applications. These applications naturally require the design of highly functional though biocompatible nanomaterials (NMs). Among the most extensively investigated NMs for biomedical imaging applications are Quantum Dots (QDs), which are semiconductor nanocrystals with a size ranging from 2 to 100 nm.[1] They possess supremely advantageous optical properties including a very high and stable fluorescence intensity that is strongly resistant to photobleaching.[2] In addition, they are known for their broad excitation spectrum and narrow emission profile enabling efficient multiplexing.[3] Based on these features QDs have been promoted as eminent materials for *in vivo* and *in vitro* biomedical applications such as tumor visualization and intracellular trafficking.[1,4–6]

With the aim to enhance the biocompatibility and optical properties of the conventional core-shell QDs, many QD designs and compositions have been investigated. Recently, gradient alloyed (GA) QDs were developed (**figure 1**).[7] The gradient structure ensures that instead of the usual size-tunable emission of conventional QDs, the emission spectra of GA-QDs can be subtly altered by adjusting their chemical composition.[8,9] This solves issues related to size limitation sometimes occurring in biological labeling and allows multiplexing of QDs without size-related changes in sensitivity.[8,10]

Despite their excellent properties, the translation of QDs in general toward biomedical applications is limited, mainly due to concerns about their toxicity. It is widely established that this toxicity, at least *in vitro*, is mainly attributed to the leaching of toxic cadmium ions and the formation of reactive oxygen species (ROS) that can induce secondary toxic effects such as DNA damage and apoptosis.[11–15] To avoid these toxic pathways, several groups are attempting to develop a more biocompatible QD core by synthesizing e.g. cadmium-free QDs.[16,17] However, next to core composition the surface chemistry of the QD can greatly influence toxicity by affecting its cellular interactions.

Several research groups have recently reported that various types of NMs can modulate (macro)autophagy.[18,19] Autophagy is a highly conserved catabolic process essential for maintaining cellular homeostasis (**figure 2**). It is usually present at a basal level in every cell where it functions as a cytoplasmic housekeeper for organelle and protein quality control. In addition, autophagy serves as a cytoprotective process that is induced to support the cell in stressful conditions such as starvation or oxidative stress.[20] Autophagy perturbations have been associated with the pathogenesis of multiple diseases including cancer, neurodegeneration and liver disease.[21–23] To date, the exact influence of cellular NM exposure on the autophagic process remains unclear. Various studies have reported clear induction of autophagy, resulting in cell death,[24] whereas others have described an inhibition on autophagosome clearance, which can also result in cell death.[25] The direct induction of cell death through the autophagy process however remains a topic of debate, as autophagy is mainly a self-preservation process and any alterations observed during cell death could simply be the result of secondary unrelated bystander effects of the cell trying to recover.[26] In line with the latter view, it has been suggested that the induction of autophagy could be beneficial, as the overall toxicity of NMs could be reduced by the protective effects of autophagy.[27,28]

Considering the impact of autophagy induction and inhibition as described above, we believe it is critical to characterize the influence of NMs on autophagy from a nanotoxicological point of view.[18] However, despite abundant reports on NM-modulated autophagy, only a few studies exist related to QDs. Furthermore, very little attention has yet been paid to the potential harm induced by the highly promising GA-QDs.[29] In addition**,** many of those studies are limited to one type of coating or lack data on intracellular uptake.[24]

In this paper we look into the influence of QD surface chemistry on the toxicity and its underlying causes by comparing two types of QDs that only differ in their coating. We opted for polyethylene glycol (PEG) as a coating, since this is the most commonly applied coating strategy in biomedical

applications to reduce unspecific protein binding and prevent aggregation. In addition, PEGylation is known to increase the blood circulation time of particles by preventing NP uptake by the reticuloendothelial system.[30–32] As a second coating strategy we selected the short ligand 3-mercaptopropionic acid (MPA) based on previous reports that observed limited toxicity with this coating.[29–31] We therefore wanted to analyze this promising observation further with a special focus on autophagy since the influence of MPA coating on this pathway remains unexplored so far. To this end, we examined the aggregation profile, cellular uptake, cytotoxicity and associated ROS levels of QDs, and studied their effect on lysosomes and autophagosomes - the two most essential organelles of the autophagy pathway.

3. METHODS

Materials

Two types of spherically shaped Gradient Alloy Quantum Dots were purchased from Mesolight LLC (Little Rock, Arkansas, USA). Both types have a gradient $CdSe_xS_{1-x}$ core surrounded by a ZnS shell. (**Figure 1**). The GA-QDs only differ in their surface coating: one particle is coated with polyethylene glycol (PEG) with terminating carboxyl groups while the other one is coated with 3-mercaptopropionic acid (MPA). Both QDs have an emission maximum at 580nm (**Supplementary Figure S1**), and exhibit very similar quantum yields, i.e. 60% for PEG-QDs and 65% for MPA-QDs. All QD dispersions were diluted from the original colloidal suspensions that were stored in H_2O with a concentration of 10 µM for PEGylated QDs (stored at pH 7) and 15 µM for MPA-coated QDs (stored at pH 11). LC3-, p62-, actin and LAMP-1-antibodies were purchased from Cell Signaling (Beverly, USA); secondary AlexaFluor® tagged antibodies, LysoTracker®, DQ™ red BSA and CellROX® were purchased from Molecular Probes™ (Invitrogen, Belgium).

Nanoparticle characterization

The hydrodynamic size and zeta potential of the QDs were determined using a Malvern Zetasizer Nano (Malvern Instruments, Worcestershire, U.K.). For this purpose the QDs were diluted to a concentration of 20 nM in HEPES buffer or Phosphate buffer saline (PBS) prior to performing the measurements at 25 °C. The refractive index was set to 2.56 based on the manufacturer's protocol (Mesolight). Size measurements were done in triplicate with three runs per replicate, and presented based on the number distribution. The zeta potentials were calculated from the electrophoretic mobility based on the Henry equation considering the Smoluchowski approximation. Zeta potential measurements were done in triplicate with two runs per replicate. The stability of both QDs in cell culture media was assessed with Single Particle Tracking of which the methodology can be found in the Supplementary information.

Cell culture

The cervical epithelial cancer cell line HeLa was purchased from ATCC (CCL-2). The stable GFP-LC3 HeLa cell line was a kind gift from Prof. Felix Randow (MRC Laboratory of Molecular Biology, Cambridge, UK). Both cell types were cultured using DMEM/F12 cell culture media (Gibco®, Paisly, UK) supplemented with 10% fetal bovine serum (Hyclone®, Cramilton, UK), 1% L-glutamine (Gibco®, Paisly, UK) and 2% penicillin – streptomycine solution (Gibco®, Paisly, UK). Cells were passaged at 80% confluency and incubated at 37°C with 5.0% CO_2.

MTT cell viability

Cells were seeded in a 96 well plate at a cell density of 20.000 cells per well. After QD treatment the medium was removed and the cells were washed twice with PBS (Gibco®, Paisly, UK). Next, fresh medium containing 5 mg/ml of MTT reagent (Sigma-Aldrich, USA) was added to the cells and incubated for 3 h at 37°C. Following this incubation, the medium was carefully removed and the formazan crystals were dissolved by incubation with DMSO on a shaker for 1 h. Finally, the absorbance was measured at 590 nm with an Envision plate reader (Perkin Elmer, Zaventem, Belgium). The percentage of viability was then calculated by comparison with untreated cells

representing 100% viability. To check for potential interference of the QDs with the MTT assay the absorbance at 590nm was also measured for several controls. The positive control (cells treated for 15 min with 0,1% Triton X-100) was compared to cells treated with QDs followed by incubation with Triton X-100. Also, culture medium containing QDs and incubated with MTT reagent was compared to culture medium only incubated with MTT reagent. In both cases, no significant change in the assay readout was detected between the controls. Cellular uptake, oxidative stress, lysosomal and autophagy markers were measured by flow cytometry. All autophagy-related studies were performed in accordance to the guidelines published by Klionsky *et al*.[36]

All flow cytometry experiments were at least performed in triplicate. For this purpose cells were seeded in a 24 well plate at a density of 60.000 cells per well. The general protocol was as follows: after 24 h of incubating the cells with QDs in full cell culture medium, the medium was removed after which a washing step with PBS was performed. Next, the cells were detached with 300 µl of 0.25% Trypsin-EDTA (Gibco®, Paisly, UK), followed by neutralizing the trypsin with 500 µl of cell culture medium and transferring the cell suspension to FACS tubes. The samples were next centrifuged at 300g for 5 min, the supernatant was removed, and the cells were resuspended in FACS buffer. This wash cycle was performed two times. Finally, the cells were resuspended in 300 µl of FACS buffer prior to analyzing them with a FACScalibur flow cytometer (BD, Erembodegem, Belgium). Data acquisition was performed with BD CellQuest™ software while the data analysis was done with Flowjo software (Tree Star Inc). The staining protocols for the respective experiments are described below.

Cellular uptake. HeLa cells were incubated with 400 µl of medium containing the respective concentrations of QDs for 24 h. After this the flow cytometry protocol as described above was executed.

LysoTracker® staining. This dye, which stains all lysosomal vesicles, was used to estimate QD-induced changes in total lysosomal content. Cells were exposed to QDs for 24 h, to 50 µM of chloroquine for

4h. After a washing step with PBS, cells were incubated with 100 nM of LysoTracker Red® DND-99 for 30 min at 37°C.

DQ™ Red BSA staining. This dye, which is degraded by the lysosomal pathway, was used to estimate QD-induced changes in the degradative capacity of lysosomes. After a 24 h incubation with QDs and a washing step with PBS the cells were treated with 10 µg/ml DQ BSA for 3 h at 37°C, allowing the endocytic uptake of the fluorescent BSA. Chloroquine-treated and starved cells were pre-incubated for 1 h with 50 µM chloroquine or serum-free medium prior to co-incubation with DQ BSA so that the total treatment was each time 4 h.

CellROX® staining. Cells were exposed to QDs for 24 h. After a washing step with PBS, cells were incubated with 5 µM of CellROX® Deep Red for 30 min at 37°C.

GFP-LC3 detection. This protocol was based on a method described by Eng *et al.*[37] Hela cells stably expressing GFP-LC3 were seeded in a 24 well plate with a density of 60.000 cells per well. The general flow cytometry protocol was followed except for the first washing step which was performed with 0.05% saponin (Sigma-Aldrich, USA) instead of PBS. This special washing step ensures that only the LC3 present on autophagosomal membranes, which is insoluble, remains intact. After the saponin washing step, two wash cycles with PBS were executed after which the samples were analyzed.

Immunofluorescence staining for LAMP-1 and LC3

For these experiments 100.000 cells were seeded in a 35mm microscopy dish, left to adhere overnight and were then treated with QDs for 24 h, or with chloroquine or serum-free medium for 4 h. After a washing step with PBS, the cells were fixed using 2% paraformaldehyde (Sigma-Aldrich, USA) for 15 min. Next, the fixative was removed and the cells were washed three times with PBS. The cells were next permeabilized by a 15 min incubation with 0.5% Tween 20 (Sigma-Aldrich, USA) in PBS. After removing the permeabilization agent the cells were washed three times with blocking buffer (5% goat serum in PBS), after which they were incubated with blocking buffer for 15 min. Adequately diluted primary rabbit antibodies were then applied to the cells and incubated for 1 h.

After washing three times with blocking buffer, the cells were incubated with Goat anti-Rabbit Alexafluor® 647 antibodies (Life Technologies, Invitrogen, Belgium) for 1 h. After two final washing steps with PBS, the samples were kept in Vectashield antifade medium (Vector Laboratories, USA) at 4° C until imaging. All the steps of the immunostaining protocol were performed at room temperature. The samples were visualized with a Sweptfield Confocal microscope (Nikon, Belgium) using a 60x oil Plan Apo objective (Nikon, Belgium). Post-image processing of the images was done using ImageJ/FIJI software (NIH).

Western Blot

For this experiment 750.000 cells were seeded in a T25 flask. After treatment, the cell medium was removed and the cells were washed twice with ice cold PBS and harvested by scraping. The cell suspension was then centrifuged for 8 min at 1100 rpm at 4°C. The supernatant was removed and the cell pellet was resuspended in RIPA buffer (Sigma-Aldrich, USA) supplemented with protease inhibitors (Sigma-Aldrich, USA). This suspension was next centrifuged at 10 000 g for 10 min at 4°C after which the supernatants were collected and kept at -80°C until use. Protein concentrations were determined using the DC™ Protein Assay (BD, Erembodegem, Belgium). For Western blotting equal amounts of protein were loaded on a 12% SDS-PAGE gel and transferred onto a PVDF membrane (BD, Erembodegem, Belgium). After the transfer the blots were blocked with 5% bovine serum albumin (Sigma-Aldrich, USA) for 1 h at room temperature after which they were incubated overnight at 4°C with the designated primary antibodies diluted in blocking buffer. Next, the blots were incubated with HRP-conjugated secondary antibody (Cell Signaling, USA) for 1 h at room temperature. Finally the blots were visualized using the Bio-Rad ImmunStar™ WesternC™ chemiluminescent kit (Biorad) on a VersaDoc™ Imaging System (Biorad).

Statistical Analysis

All experiments were analyzed for statistical significance with a one-way ANOVA followed by the Bonferroni post hoc test to estimate significance between treated groups, or followed by the

Dunnett post hoc test when compared to an untreated group. The results were considered as statistically significant if $p < 0.05$. All statistical analysis was performed with Graphpad Prism 5 software (San Diego, CA).

4. RESULTS

Quantum Dot characterization

As described in **Figure 3**, DLS measurements have shown that both QDs exhibit similar size (~20 nm) and zeta potential (~ -22 mV) in HEPES buffer. A negative zeta potential could be expected for both QDs since MPA is a strong acid and the PEG chains have carboxyl end groups. To characterize the QDs in an ion-rich solution (similar to cell medium) we examined their size and zeta potential in PBS. In this buffer, the PEGylated QDs remain stable (~20 nm), however, the MPA-coated ones form aggregates (**Figure 3A**). In PBS the charge of PEGylated QDs is neutralized to -10 mV while MPA-coated QDs exhibit similar charge as in HEPES buffer, being -22 mV (**Figure 3B**). As expected, exposure to cell culture medium elicited a similar trend as in PBS: PEGylated QDs show an uniform size distribution while MPA-QDs clearly aggregate as indicated by their very broad size distribution. (**Supplementary Figure S2**).

Uptake and intracellular localization of Quantum Dots

Uptake experiments (**Figure 4**) showed that PEGylated QDs are easily taken up at low concentrations, though the uptake does reach a plateau around 40 nM and decreases at concentrations above 60 nM. In contrast, MPA QDs are only efficiently taken up starting from a concentration of 80 nM, and their uptake increases proportionally to the administered dose. In order to study the intracellular effects later on, we continued our study with dosages of the two types of QDs that should result in comparable intracellular concentrations. Considering the similar quantum yield of both QDs we compared dosages that gave an identical average fluorescence intensity per cell, i.e. 20 nM PEG QDs and 125 nM MPA QDs, as well as 50 nM of PEG QDs and 175 nM of MPA QDs.

As discussed in more detail later, **Figure 6** shows that both QDs accumulate in the perinuclear region and co-localize strongly with lysosomes, indicating that both particles are taken up by endocytosis.

Quantum Dot-induced acute toxicity and oxidative stress

QD-induced cytotoxicity was determined based on reduction in cellular enzymatic activity. This was tested using the common MTT viability assay after a QD incubation for 24 h for a concentration range up to 200 nM. As shown in **Figure 5A**, MPA QDs did not evoke significant toxicity over the tested concentration range. In contrast, PEGylated QDs clearly elicited a dose dependent toxicity with a significant decrease in cell viability ranging from 80.6% (± 1.8) viability at 50 nM to 33.7% (± 1.2) viability at 200 nM. Next to enzymatic activity, we also determined cytotoxicity based on cell membrane rupture by measuring propidium iodide uptake. Again, exposure to 50 nM of PEGylated QDs led to a significant decrease in viability while MPA-QDs induced no cell death up to 175 nM (**Supplementary Figure S3**). The level of ROS, a measure for oxidative stress, was determined by incubation of QD treated cells with CellROX®, a dye that becomes fluorescent after oxidation by ROS. As shown in **Figure 5B**, a 24 h exposure of HeLa cells to PEGylated QDs gives rise to significantly higher levels of ROS: 123 (±4.3) % for 20 nM and 135 (±4.0)% for 50 nM. Remarkably, in case of MPA QDs the oxidative stress level decreased, as the ROS levels were significantly reduced to 85 (±4.5)% and 76 (± 5.1)% for 125 nM and 175 nM respectively.

Impact of Quantum Dots on lysosomal health

Until recently the lysosome was merely considered as the waste bag of the cell, since it degrades and recycles the content delivered to the lysosomal compartment following endocytosis or autophagy. However, thanks to recent reports further elucidating its functions the lysosome is now more and more perceived as an essential organelle for protecting the cell's homeostasis.[38] To our interest, its activity is also crucial to ensure a functional autophagy pathway (**Figure 2**). Therefore, we evaluated the effect of QDs on lysosomal abundance and functionality by flow cytometry (indicated in **Figure 6**).

As a first indication, we incubated QD treated cells with LysoTracker, a dye that accumulates in lysosomes, and followed its intensity with flow cytometry as a measure for the amount and/or size of the lysosomal network.[39] As a positive control we treated the HeLa cells with 50 µM of chloroquine for 4h, since it is widely established that this buffer elicits alkalinization of the lysosomal lumen which next evokes lysosomal swelling.[40] As shown in **Figure 6A**, this treatment indeed led to an almost twofold increase (194 ±14%) in LysoTracker intensity. A 24 h incubation with 20 and 50 nM PEGylated QDs resulted in an even more substantial increase up to 240 (±15)% and 248 (± 24)% respectively. The rise in LysoTracker intensity for the MPA coated QDs was not as spectacular as for their PEGylated counterparts though a significant dose-dependent effect was apparent: 125 nM led to 162 (± 14)% while 175 nM gave rise to 220 (± 26)%.

To support this data we performed confocal microscopy on cells stained for LAMP-1, a lysosomal membrane marker.[41] As illustrated in **Figure 6B** some lysosomes of chloroquine-treated cells appeared as swollen compared to those of untreated cells, which supports the rise in LysoTracker intensity seen with flow cytometry. Instead, confocal images show that the increase in LysoTracker intensity in QD-treated cells seems rather due to an increase in the number of lysosomes. Moreover, we noticed there was a strong co-localization between lysosomes and both types of QDs, illustrating that both QDs were taken up by endocytosis and thus efficiently delivered to the lysosomal compartment.

Finally, we examined the functionality of lysosomes of cells exposed to QDs, *i.e*. their ability of degrading lysosomal content. To this end, HeLa cells were incubated with the Derivatively Quenched Bovine Serum Albumin (DQ BSA) dye which consists of BSA proteins that are heavily labeled with fluorescent dyes so that a strong quenching effect takes place. Upon (lysosomal) degradation of DQ BSA into smaller fragments, this quenching effect is abolished, resulting in a bright fluorescent signal. In other words, an increase in fluorescence represents an increase in lysosomal protein degradation. As a positive control for increased lysosomal activity, cells were incubated for 4 hours with serum-

free medium to mimic starvation. **Figure 6C** demonstrates that this treatment indeed gave rise to a substantial increase in DQ BSA fluorescence (176 ±14%). This in stark contrast to chloroquine-treated cells where the protein degradation capacity was almost halved (54 ±2.9%). This is not surprising since it has repeatedly been reported that starvation and chloroquine result in upregulation of lysosomal activity and lysosomal impairment, respectively.[42,43] Indeed, the alkalinization of lysosomal pH induced by chloroquine inhibits the degradative enzymes that are in need of an acidic environment. On the other hand, starvation stimulates lysosomal activity and autophagy as the cell attempts to compensate for the nutrient deficit.[44,45] For the QDs, the effect on lysosomal degradation strongly depended on the type of coating. No substantial change in degradation was observed upon treatment with PEGylated QDs. MPA QDs, however, did result in significant enhancement of DQ BSA fluorescence up to 134 (± 5.4)% with 175 nM. This signifies that MPA-QD uptake results in a starvation-like activation of lysosomal degradative capacity.

Impact of Quantum Dots on autophagy

Next, we focused on the most important organelle of the autophagy pathway *i.e* the autophagosome. The most widely investigated marker for autophagosomes is the protein LC3 (Microtubule Associated Protein 1 Light Chain 3), which is present as two forms within the cell: the unactivated form, LC3-I, which is present in the cytosol and the active form LC3-II that is incorporated into the autophagosomal membrane **(figure 2)**. Consequently, the autophagy pathway can be studied by following the processing of LC3. To reliably interpret changes in autophagy, we inspected LC3 by multiple techniques including (i) flow cytometry on HeLa cells stably expressing GFP-LC3 and (ii) western blotting on autophagosomal markers. As a first indication the level of GFP-LC3 was quantified by flow cytometry in a stably transfected GFP-LC3 HeLa cell line. When autophagosomes fuse with lysosomes the GFP will be quenched by the acidic pH.[44,46] The fluorescence intensity level of GFP is therefore proportional to the amount of autophagosomes. Furthermore, the saponin extraction included in the sample preparation ensures that only the membrane-bound LC3 contributes to the detected signal.[37] A 4h incubation with 50 µM of chloroquine was applied as a

positive control for autophagosome accumulation throughout all autophagy experiments. The lysosomal impairment caused by chloroquine leads to a block in autophagosome-lysosome fusion which results in the accumulation of large autophagosomes positive for LC3-II (see Figure 2).[44] Indeed, as shown in **Figure 7A**, chloroquine treatment resulted in more than a three-fold increase in GFP-LC3 fluorescence intensity compared to untreated cells (342 ±60%). Interestingly, the highest concentration of PEGylated QDs gave rise to a significant increase in GFP-LC3 (175 ±26%) while MPA QD treatment did not.

To support this data we performed confocal microscopy on HeLa cells stained for LC3 after treatment with PEG QDs , MPA QDs or chloroquine. Here, the confocal images in **Figure 7B** show that chloroquine-treated cells contain some larger autophagosomes compared to untreated cells. In case of PEG QD treatment the total autophagosomal content seemed higher. In contrast, MPA QD treatment did not appreciably affect autophagosomal abundance nor size. It should be noted that for both QDs there was little co-localization with autophagosomes. Since the QDs are not present in the cytosol the only way of entering the autophagy pathway would be via fusion of autophagosomes with QD-containing lysosomes. Seeing the lack of co-localization we can conclude that these fusion events do not take place.

As mentioned in **Figure 2**, the level of p62 is often studied to determine if the overall autophagy pathway is entirely functional. Since p62 is solely degraded by autophagy, a rise or fall of its protein level compared to the untreated condition corresponds with an autophagy blockade or upregulation respectively.[47] **Figure 7C** shows the protein levels of p62 and LC3 as determined by Western blotting. Interestingly, the level of p62 was higher for cells treated with 50 nM of PEGylated QDs. As expected based on our observations by microscopy and flow cytometry, a higher level of LC3-II was spotted upon incubation with PEGylated QDs at 50 nM. The rise in LC3-II induced by chloroquine was even more pronounced. In contrast, no change in both markers was detected upon incubation of HeLa cells with MPA-coated QDs.

5. Discussion

In this study we apply a step-by-step approach to carefully examine the toxicity of QDs coated with two commonly applied surface ligands. Our data clearly accentuates that the choice of coating is crucial for the degree and mechanisms of toxicity induced by QDs on cells: while MPA coated QDs were highly biocompatible, PEGylated QDs were severely toxic at higher concentrations. A detailed investigation of the ROS production, lysosomal health and autophagy pathway gave some insight in the intracellular mechanisms that could account for these observations.

MPA coated QDs

Coating of QDs with the short ligand MPA was not sufficient to protect the particles from aggregation in buffer or cell culture medium. The aggregated particles were taken up efficiently, though only at higher concentrations. This could be expected since it has been observed before that NP agglomeration has a negative impact on cellular uptake.[48–50] It is therefore likely that we need a higher dosage of MPA-coated QDs to reach similar intracellular fluorescence levels as PEGylated QDs because only the smaller NPs of the dispersion of MPA-QDs are able of entering the cells.[51] Interestingly, Albanese *et al.* stated that the effect of particle aggregation on uptake might be cell-type dependent: gold nanoparticle aggregation led to a reduced uptake in HeLa cells while for a melanoma cell type the opposite was true.[49] In any case, despite the efficient uptake of MPA-QDs, they did not inflict any toxicity on HeLa cells. This biocompatibility corresponds with the findings of Nagy et al. who did not detect any cell death in primary human lung cells upon exposure to differently sized MPA-coated QDs, though they did not show any uptake data.[34] Soenen *et al.*, however, did detect significant toxicity with MPA-coated QDs starting from 50 nM.[29] This difference with our data may be attributed to differences in aggregation: their MPA-QDs form smaller aggregates, which could lead to more efficient uptake and consequently toxicity at lower concentrations. This hypothesis was confirmed *in vivo* in mice where aggregated MPA-QDs exhibited

less toxicity than their unaggregated counterparts.[52] On the other hand, the discrepancy in toxicity could also be derived from cell type dependent effects.[53,54]

The most recognized mechanism of QD-induced toxicity is the production of reactive oxygen species (ROS).[55] Shifting ROS levels can indeed lead to a variety of secondary effects such as changes in cell signaling and DNA damage.[15] In addition, ROS and oxidative stress are associated with multiple cell death pathways and have been identified as important regulators of autophagy.[56–58] Strikingly, incubation with MPA-coated QDs led to a significant reduction in ROS levels (**Fig. 5B**)**.** Though this observation was unexpected, an NM-induced reduction in ROS has been reported before.[59] Specifically regarding QDs, studies have until now only reported that there is a lack of ROS induction by MPA-coated QDs.[34,35]

Apart from ROS levels, we looked further into the impact of QD exposure on lysosomal health and autophagy. As a first step we evaluated the influence of QDs on the number and size of lysosomes. Here we found that treatment of HeLa cells with MPA-coated QDs elicited a significant expansion of the lysosomal compartment as indicated by the substantially increased levels of LysoTracker. This type of enlargement is a commonly reported phenomenon and has been described for various NMs including ZnO NPs, fullerenol NPs, polystyrene NPs and QDs.[27,60–62] Interestingly, the increase in lysosomal content was accompanied by a rise in cellular degradation capacity, which is an indication for lysosomal activation. A boost in protein degradation was also observed by Chen *et al.* who, similar to our findings, detected an increase in LysoTracker staining and DQ BSA degradation upon treatment of human cerebral microvascular endothelial cells with aluminum nanoparticles.[63] In addition, Kenzaoui *et al*. observed lysosomal activation induced in brain-derived endothelial cells by multiple NMs such as iron oxide NPs and silica NPs.[64] This kind of lysosomal activation, as caused by our MPA-coated QDs, is often accompanied by a similar activation of autophagy. However, the unaltered level of p62 and LC3 indicates that the autophagy pathway is fully functional though at a basal level. Similar to autophagy induction, this QD-induced lysosomal activation likely aids the cell in

overcoming stress. In combination with the reduced oxidative stress, this could explain the lack of toxicity we observed upon exposure of HeLa cells to these QDs. Our findings thus confirm that MPA-coated QDs are quite biocompatible. Furthermore, our group recently reported that cells labeled with GA-QDs can be tracked 1.5 times longer than conventional core-shell QDs.[29] In conclusion, the combination of this excellent functionality and biocompatibility makes these MPA-coated GA-QDs very well suited for cell labeling applications.

PEGylated QDs

Unlike MPA coated QDs, PEGylated QDs do not agglomerate in ion-rich media, most likely due to the steric hindrance imparted by the PEG-chains which prevents particle-particle interactions.[65] As Pelaz *et al.* stated, PEGylation more than often leads to a reduction in cellular uptake which is likely attributed to the lack of protein adsorption at the particle surface.[66] On the other hand, the colloidal stability of our particles likely supports their uptake as stated before by Kirchner *et* al.[51,67] Indeed the smaller and more neutral PEGylated QDs were clearly taken up more efficiently (even at lower extracellular concentrations) than the larger negatively charged MPA-coated QDs. Starting from 60 nM, however, the uptake of PEGylated QDs shows a downward trend. An explanation for this decrease in uptake might be the saturation of surface receptors essential for QD uptake, since it has been described before that neutral to negatively charged QDs are actively internalized by a variety of saturable endocytosis pathways including clathrin- and caveolae-mediated endocytosis.[68,69] Upon investigation of the intracellular location of both QDs we indeed found that after 24h they co-localize strongly with LAMP-1 stained lysosomes implying they are taken up via endocytosis. The decreased uptake of PEGylated QDs upon treatment with higher concentrations could also stem from QD-induced toxicity, as cytotoxicity tests revealed that PEGylated QDs were significantly toxic starting from 50 nM.

Regarding QDs, a common strategy to prevent ROS induction is to limit the dissolution of cadmium ions from their core by the application of a surface coating.[51] Clearly, high density PEGylation is not

sufficient to prevent ROS production since exposure to 50 nM of PEGylated QDs significantly raised the level of ROS in HeLa cells. Since this observation correlates well with the cell death seen at this concentration, we suggest this ROS production is at least partly responsible for the observed cytotoxicity. In addition, these findings correspond well with the many reports on QD-induced cell death associated with oxidative stress.[12,29,70] However, not only does the coating influence the dissolution of ions from the NP core, the coating itself can also exert ROS generation. This was observed by Soenen *et al.* who found that at identical cellular NP levels, PEGylated gold NPs were more toxic than non-PEGylated ones, indicating that PEG provokes ROS generation.[67] In any case, the difference in toxicity observed between the PEG- and MPA-coated QDs demonstrates that the type of surface functionalization can have a marked influence on the toxicity and ROS production of QDs. This observation was also made by Nagy *et al.*, who observed less QD-induced toxicity with shorter negatively charged surface ligands compared to longer ligands - in our case represented by MPA and PEG respectively.[34]

With regard to the lysosomes, also PEGylated QDs resulted in an enlargement of the lysosomal compartment. Interestingly, despite the fact that PEGylated QDs give rise to a more than twofold increase in LysoTracker, the degradation of DQ BSA did remain unchanged. We therefore suspect that at least a part of these lysosomes exhibit limited or no proteolytic activity and thus these QDs lead to lysosomal impairment. Lysosomal impairment is a frequently described mechanism of toxicity in cells exposed to various NMs as summarized in a review by Stern et al.[71] The most extensively reported mechanism of lysosomal impairment involves lysosome membrane permeabilization. However, considering the high LysoTracker dye loading and LAMP-1 staining showing normal lysosomal morphology, we believe that in our case the lysosomal membrane is intact. We therefore hypothesize that the mechanism underlying this impairment could be lysosomal overload as has previously been reported for several particles such as smoke particulates.[71,72] Another mechanism that could contribute to the lack of degradation taking place within the lysosomes could be oxidative damage inflicted on the lysosomal enzymes by ROS produced during QD lysis.[71] By any means,

lysosomal dysfunction is undeniably a toxic parameter worth of investigation since it forms the basis of lysosomal storage disorders, a group of degenerative diseases that affect the nervous and musculoskeletal systems. In addition, lysosomal malfunction can give rise to an autophagy blockade through impaired autophagosome-lysosome fusion, a hypothesis we investigated further.[73]

When looking into autophagosomal markers, treatment of HeLa cells with 50 nM of PEGylated QDs resulted in an elevation of LC3, indicative of an accumulation of autophagosomes. Since the p62 protein level was also increased, we conclude that the accumulation of LC3 derives from a reduction in autophagosomal turn-over rather than autophagy induction. In other words, the autophagy pathway is not fully functional but blocked at its later stage i.e. at autophagosome-lysosome fusion **(Figure 2)**. Since no co-localization of QDs with autophagosomes was observed (**Figure 7**), we conclude from this collection of data that PEGylated QDs induce autophagosome accumulation through lysosomal impairment.

This theory is in line with observations made by Ma *et al*. who detected compromised degradation capacity induced by endocytosed AuNPs and consequently defective autophagosome-lysosome fusion in normal rat kidney cells.[25] An impaired autophagy flux was also hypothesized by Wang *et al.* who witnessed an increase in the volume of acidic compartments and LC3-II levels upon exposure of human brain astrocytoma cells to polystyrene particles.[62] In addition, the same conclusion was drawn based on similar observations in kidney cells treated with fullerenol NPs.[61] At first sight our findings do seem in contrast with recent observations made by Huang *et al* who saw that NPs modulate autophagy in a dispersity-dependent manner where aggregated NPs induced severe autophagic effects while well-dispersed NPs did not.[74] Our study indicates that MPA-QDs, which aggregate severely in extracellular medium, do not exert major effects on the autophagy pathway while our unaggregated PEGylated QDs clearly do. However, within the cell this phenomenon might be the opposite: as stated before it is likely that the large MPA-QD aggregates are not internalized by the cell while the smaller PEGylated QDs are taken up very efficiently and likely accumulate, and

possibly aggregate, massively inside the endo- and lysosomes. According to Huang *et al.* this high uptake and intracellular accumulation of NPs can next modulate autophagy, which is in line with our observations.Since autophagy usually encourages survival, especially in cells undergoing stress, it is not surprising that when this function is lost, cytotoxicity becomes inevitable.[75] Our PEGylated QDs induce oxidative stress that undoubtedly leads to damaged cytoplasmic material. Where usually autophagy aids in the removal of these materials, this coping mechanism is now absent. The autophagy blockade combined with oxidative stress is therefore likely the underlying source of the QD-induced cytotoxicity we observed. This disrupted autophagy flux is a serious observation since this can lead to the accumulation of protein aggregates and damaged cytoplasmic organelles. This buildup of cytoplasmic waste can subsequently provoke genomic instability and tissue degeneration, which in turn has a huge impact on physiology.[21] Surely, autophagy dysfunction is linked with the onset of many diseases including cancer, neurodegenerative and inflammatory diseases.[21,76]

However, autophagy perturbation should not be regarded as threatening per se. Actually, in distinct cases it can be manipulated to our advantage. Recent reports have stated that inducing autophagy malfunction might be an ideal strategy to wipe out (resistant) cancer cells. It seems some types of cancer are highly dependent on autophagy for their survival, since autophagy allows them to overcome stressors like starvation, hypoxia and even chemotherapy.[18,23] Blocking this cytoprotective process would in this case thus lead to their demise. In fact, the anti-cancer activity of chloroquine, a chemical we use as a positive control for autophagy blockade, is currently investigated in multiple clinical trials.[77] In this regard, the effects induced by PEGylated QDs might allow us to combine diagnosis by tumor imaging with anti-cancer therapy. In conclusion, the oxidative stress and autophagy blockade caused by these PEGylated GA-QDs has detrimental effects for the cell, however, in cases where these effects are desirable like in anti-cancer therapy, these particles could be valuable.

6. Conclusion

The primary goal of this study was to define the toxicity and its origins of MPA-coated and PEGylated QDs with a special emphasis on the autophagy pathway. We observed that despite the fact the two studied QDs are completely identical except for their surface coating, their cellular effects induced in HeLa cells were remarkably different (**Figure 8**). This implies that rather than QD composition, the surface chemistry primarily defines the functionality and toxicity of the QD. Based on our results we conclude that MPA-coated QDs are highly biocompatible, where the lysosomal activation and ROS reduction induced by these QDs likely rescues the cell from potentially NM-induced toxic effects. In this respect, MPA-coated QDs seem promising candidates for cellular labeling. However, since this study is limited by its focus on ROS and autophagy, future research should involve screening for other toxic factors such as DNA damage. As expected, the PEGylated QDs proved to be more resistant to aggregation resulting in efficient cell labeling. However, these QDs exhibited significant toxicity owing to their capacity to induce ROS production and autophagy malfunction through lysosomal impairment. Considering these toxic defects, the PEGylated QDs do not seem suitable for biomedical applications except for when autophagy dysfunction is actually desirable e.g. in anti-cancer therapy. In this regard, it could be valuable to investigate if combination therapy using a common chemotherapeutic and this QD might enhance the elimination of therapy-resistant cancer cells. Generally, our study highlights the importance of surface chemistry when it comes to nanotoxicology as well as the relevance of lysosomal and autophagy dysfunction as a nanomaterial-induced toxicity mechanism.

7. Acknowledgements

This project has been funded by the Institute for the Promotion of Innovation through Science and Technology in Flanders, Belgium (IWT – Vlaanderen). SJS is supported for the FWO-Vlaanderen. We acknowledge Prof. Felix Randow for providing the GFP-LC3 labeled HeLa cell line. We would also like to thank professor Dieter Deforce for the use of the VersaDoc™ Imaging System.

8. Conflict of Interest

The authors declare that they have no competing interests.

9. References

[1] T.L. Doane, C. Burda, The unique role of nanoparticles in nanomedicine: imaging, drug delivery and therapy, Chem. Soc. Rev. 41 (2012) 2885–2911.

[2] M.-X. Zhao, E.-Z. Zeng, Application of functional quantum dot nanoparticles as fluorescence probes in cell labeling and tumor diagnostic imaging., Nanoscale Res. Lett. 10 (2015) 171.

[3] W.C.W. Chan, D.J. Maxwell, X.H. Gao, R.E. Bailey, M.Y. Han, S.M. Nie, Luminescent quantum dots for multiplexed biological detection and imaging, Curr. Opin. Biotechnol. 13 (2002) 40–46.

[4] C.M. Hessel, V.P. Pattani, M. Rasch, M.G. Panthani, B. Koo, J.W. Tunnell, B.A. Korgel, Copper selenide nanocrystals for photothermal therapy., Nano Lett. 11 (2011) 2560–6.

[5] T.M. Samir, M.M.H. Mansour, S.C. Kazmierczak, H.M.E. Azzazy, Quantum dots: heralding a brighter future for clinical diagnostics., Nanomedicine (Lond). 7 (2012) 1755–69.

[6] C.E. Probst, P. Zrazhevskiy, V. Bagalkot, X. Gao, Quantum dots as a platform for nanoparticle drug delivery vehicle design, Adv Drug Deliv Rev. 65 (2013) 703–718.

[7] W.K. Bae, L.A. Padilha, Y.-S. Park, H. McDaniel, I. Robel, J.M. Pietryga, V.I. Klimov, Controlled alloying of the core-shell interface in CdSe/CdS quantum dots for suppression of Auger recombination., ACS Nano. 7 (2013) 3411–9.

[8] R.E. Bailey, S. Nie, Alloyed semiconductor quantum dots: tuning the optical properties without changing the particle size., J. Am. Chem. Soc. 125 (2003) 7100–6.

[9] G.I. Maikov, R. Vaxenburg, A. Sashchiuk, E. Lifshitz, Composition-Tunable Optical Properties with Alloy Components, ACS Nano. 4 (2010) 6547–6556.

[10] Mesolight, http://www.mesolight.com/e/list.php?classid=23, (n.d.).

[11] K.M. Tsoi, Q. Dai, B.A. Alman, W.C.W. Chan, Are quantum dots toxic? Exploring the discrepancy between cell culture and animal studies, Acc. Chem. Res. 46 (2012) 662–671.

[12] J. Lovrić, S.J. Cho, F.M. Winnik, D. Maysinger, Unmodified cadmium telluride quantum dots induce reactive oxygen species formation leading to multiple organelle damage and cell death., Chem. Biol. 12 (2005) 1227–34.

[13] A. Al-Ali, N. Singh, B. Manshian, T. Wilkinson, J. Wills, G.J.S. Jenkins, S.H. Doak, Quantum dot induced cellular perturbations involving varying toxicity pathways, Toxicol. Res. (Camb). (2015).

[14] N. Chen, Y. He, Y. Su, X. Li, Q. Huang, H. Wang, X. Zhang, R. Tai, C. Fan, The cytotoxicity of cadmium-based quantum dots., Biomaterials. 33 (2012) 1238–44.

[15] K.T. Yong, W.C. Law, R. Hu, L. Ye, L. Liu, M.T. Swihart, P.N. Prasad, Nanotoxicity assessment of quantum dots: from cellular to primate studies, Chem. Soc. Rev. (2013).

[16] T. Pons, E. Pic, N. Lequeux, E. Cassette, L. Bezdetnaya, F. Guillemin, F. Marchal, B. Dubertret, Cadmium-free CuInS2/ZnS quantum dots for sentinel lymph node imaging with reduced toxicity., ACS Nano. 4 (2010) 2531–8.

[17] S.J. Soenen, B.B. Manshian, T. Aubert, U. Himmelreich, J. Demeester, S.C. De Smedt, Z. Hens, K. Braeckmans, Cytotoxicity of Cadmium-Free Quantum Dots and Their Use in Cell Bioimaging, Chem. Res. Toxicol. (2014).

[18] K. Peynshaert, B.B. Manshian, F. Joris, K. Braeckmans, S.C. De Smedt, J. Demeester, S.J. Soenen, Exploiting Intrinsic Nanoparticle Toxicity: The Pros and Cons of Nanoparticle-Induced Autophagy in Biomedical Research., Chem. Rev. 114 (2014) 7581–7609.

[19] K. Remaut, V. Oorschot, K. Braeckmans, J. Klumperman, S.C. De Smedt, Lysosomal capturing of cytoplasmic injected nanoparticles by autophagy: An additional barrier to non viral gene delivery, J. Control. Release. (2014).

[20] L. Li, Y. Chen, S.B. Gibson, Starvation-induced autophagy is regulated by mitochondrial reactive oxygen species leading to AMPK activation., Cell. Signal. 25 (2013) 50–65.

[21] B. Levine, G. Kroemer, Autophagy in the pathogenesis of disease, Cell. 132 (2008) 27–42.

[22] F.M. Menzies, A. Fleming, D.C. Rubinsztein, Compromised autophagy and neurodegenerative diseases, Nat. Rev. Neurosci. 16 (2015) 345–357.

[23] E. White, The role for autophagy in cancer., J. Clin. Invest. 125 (2015) 42–6.

[24] K. Peynshaert, B.B. Manshian, F. Joris, K. Braeckmans, S.C. De Smedt, J. Demeester, S.J. Soenen, Exploiting Intrinsic Nanoparticle Toxicity: The Pros and Cons of Nanoparticle-Induced Autophagy in Biomedical Research, Chem. Rev. 114 (2014) 7581–7609.

[25] X. Ma, Y. Wu, S. Jin, Y. Tian, X. Zhang, Y. Zhao, L. Yu, X.-J. Liang, Gold Nanoparticles Induce Autophagosome Accumulation through Size-Dependent Nanoparticle Uptake and Lysosome Impairment, ACS Nano. 5 (2011) 8629–8639.

[26] G. Kroemer, B. Levine, Autophagic cell death: the story of a misnomer, Nat. Rev. Mol. Cell Biol. 9 (2008) 1004–1010.

[27] K.D. Neibert, D. Maysinger, Mechanisms of cellular adaptation to quantum dots - the role of glutathione and transcription factor EB, Nanotoxicology. 6 (2012) 249–262.

[28] Y.H. Luo, S.B. Wu, Y.H. Wei, Y.C. Chen, M.H. Tsai, C.C. Ho, S.Y. Lin, C.S. Yang, P. Lin, Cadmium-

based quantum dot induced autophagy formation for cell survival via oxidative stress, Chem. Res. Toxicol. 26 (2013) 662–673.

[29] S.J. Soenen, B.B. Manshian, U. Himmelreich, J. Demeester, K. Braeckmans, S.C. De Smedt, The performance of gradient alloy quantum dots in cell labeling., Biomaterials. 35 (2014) 7249–58.

[30] H. Hatakeyama, H. Akita, H. Harashima, The Polyethyleneglycol Dilemma: Advantage and Disadvantage of PEGylation of Liposomes for Systemic Genes and Nucleic Acids Delivery to Tumors, Biol. Pharm. Bull. 36 (2013) 892–899.

[31] J. V Jokerst, T. Lobovkina, R.N. Zare, S.S. Gambhir, Nanoparticle PEGylation for imaging and therapy., Nanomedicine (Lond). 6 (2011) 715–28.

[32] J. Lipka, M. Semmler-Behnke, R.A. Sperling, A. Wenk, S. Takenaka, C. Schleh, T. Kissel, W.J. Parak, W.G. Kreyling, Biodistribution of PEG-modified gold nanoparticles following intratracheal instillation and intravenous injection., Biomaterials. 31 (2010) 6574–81.

[33] C. Kirchner, T. Liedl, S. Kudera, T. Pellegrino, A. Muñoz Javier, H.E. Gaub, S. Stölzle, N. Fertig, W.J. Parak, Cytotoxicity of colloidal CdSe and CdSe/ZnS nanoparticles., Nano Lett. 5 (2005) 331–8.

[34] A. Nagy, A. Steinbrück, J. Gao, N. Doggett, J.A. Hollingsworth, R. Iyer, Comprehensive Analysis of the effects of CdSe quantum dot size, surface charge, and functionalization on primary human lung cells, ACS Nano. 6 (2012) 4748–4762.

[35] A. Nagy, J.A. Hollingsworth, B. Hu, A. Steinbrueck, P.C. Stark, C.R. Valdez, M. Vuyisich, M.H. Stewart, D.H. Atha, B.C. Nelson, R. Iyer, Functionalization-Dependent Induction of Cellular Survival Pathways by CdSe Quantum Dots in Primary Normal Human Bronchial Epithelial Cells, ACS Nano. 7 (2013) 8397–8411.

[36] Z.S. Klionsky DJ, Abdelmohsen K, Abe A, Abedin MJ, Abeliovich H, Acevedo Arozena A, Adachi H, Adams CM, Adams PD, Adeli K, Adhihetty PJ, Adler SG, Agam G, Agarwal R, Aghi MK, Agnello M, Agostinis P, Aguilar PV, Aguirre-Ghiso J, Airoldi EM, Ait-Si-Ali S, Akemat, Guidelines for use and interpretation of assays for monitoring autophagy (3rd edition), Autophagy. 12 (2016) 1–222.

[37] K.E. Eng, M.D. Panas, G.B.K. Hedestam, G.M. McInerney, A novel quantitative flow cytometry-based assay for autophagy, Autophagy. 6 (2010) 634–641.

[38] H. Appelqvist, P. Waster, K. Kagedal, K. Ollinger, The lysosome: from waste bag to potential therapeutic target, J. Mol. Cell Biol. 5 (2013) 214–226.

[39] B.W. Neun, S.T. Stern, Monitoring lysosomal activity in nanoparticle-treated cells, Methods Mol Biol. 697 (2011) 207–212.

[40] V.R. Solomon, H. Lee, Chloroquine and its analogs: a new promise of an old drug for effective and safe cancer therapies., Eur. J. Pharmacol. 625 (2009) 220–33.

[41] E.-L. Eskelinen, Y. Tanaka, P. Saftig, At the acidic edge: emerging functions for lysosomal membrane proteins, Trends Cell Biol. 13 (2003) 137–145.

[42] J. Zhou, S.-H. Tan, V. Nicolas, C. Bauvy, N.-D. Yang, J. Zhang, Y. Xue, P. Codogno, H.-M. Shen, Activation of lysosomal function in the course of autophagy via mTORC1 suppression and autophagosome-lysosome fusion., Cell Res. 23 (2013) 508–23.

[43] M. Li, B. Khambu, H. Zhang, J.-H. Kang, X. Chen, D. Chen, L. Vollmer, P.-Q. Liu, A. Vogt, X.-M. Yin, Suppression of Lysosome Function Induces Autophagy via a Feedback Down-regulation of MTOR Complex 1 (MTORC1) Activity, J. Biol. Chem. 288 (2013) 35769–35780.

[44] N. Mizushima, T. Yoshimori, B. Levine, Methods in Mammalian Autophagy Research, Cell. 140 (2010) 313–326.

[45] C. Settembre, C. Di Malta, V.A. Polito, M. Garcia-Arencibia, F. Vetrini, S. Erdin, S.U. Erdin, T. Huynh, D. Medina, P. Colella, M. Sardiello, D.C. Rubinsztein, A. Ballabio, TFEB Links Autophagy to Lysosomal Biogenesis, Science 332 (2011) 1429–1433.

[46] E.T.W. Bampton, C.G. Goemans, D. Niranjan, N. Mizushima, A.M. Tolkovsky, The dynamics of autophagy visualized in live cells - From autophagosome formation to fusion with endo/lysosomes, Autophagy. 1 (2005) 23–36.

[47] G. Bjørkøy, T. Lamark, A. Brech, H. Outzen, M. Perander, A. Overvatn, H. Stenmark, T. Johansen, p62/SQSTM1 forms protein aggregates degraded by autophagy and has a protective effect on huntingtin-induced cell death., J. Cell Biol. 171 (2005) 603–14.

[48] B.B. Manshian, S.J. Soenen, A. Brown, N. Hondow, J. Wills, G.J.S. Jenkins, S.H. Doak, Genotoxic capacity of Cd/Se semiconductor quantum dots with differing surface chemistries, Mutagenesis. 31 (2016) 97–106.

[49] A. Albanese, W.C.W. Chan, Effect of Gold Nanoparticle Aggregation on Cell Uptake and Toxicity BT - ACS Nano, ACS Nano. 5 (2011) 5478–5489.

[50] B.D. Chithrani, A.A. Ghazani, W.C.W. Chan, Size and Shape Dependence of Nanoparticles on Cellular Uptake, Nano. 668 (2006) 662–668.

[51] C. Kirchner, T. Liedl, S. Kudera, T. Pellegrino, A. Muñoz Javier, H.E. Gaub, S. Stölzle, N. Fertig, W.J. Parak, Cytotoxicity of colloidal CdSe and CdSe/ZnS nanoparticles, Nano Lett. 5 (2005) 331–338.

[52] Y.F. Loginova, N.I. Kazachkina, V. V Zherdeva, A.L. Rusanov, M. V Shirmanova, E. V Zagaynova, E.A. Sergeeva, S. V Dezhurov, M.S. Wakstein, A.P. Savitsky, Biodistribution of intact fluorescent CdSe/CdS/ZnS quantum dots coated by mercaptopropionic acid after intravenous injection into mice, J. Biophotonics. 5 (2012) 848–859.

[53] F. Joris, B.B. Manshian, K. Peynshaert, S.C. De Smedt, K. Braeckmans, S.J. Soenen, Assessing nanoparticle toxicity in cell-based assays: influence of cell culture parameters and optimized models for bridging the in vitro–in vivo gap, Chem. Soc. Rev. 42 (2013) 8339–8359.

[54] S.K. Sohaebuddin, P.T. Thevenot, D. Baker, J.W. Eaton, L. Tang, Nanomaterial cytotoxicity is composition, size, and cell type dependent., Part. Fibre Toxicol. 7 (2010) 22.

[55] F.M. Winnik, D. Maysinger, Quantum Dot Cytotoxicity and Ways To Reduce It, Acc Chem Res. 46 (2013) 672–680.

[56] Y. Chen, E. McMillan-Ward, J. Kong, S.J. Israels, S.B. Gibson, Oxidative stress induces autophagic cell death independent of apoptosis in transformed and cancer cells, Cell Death Differ. 15 (2008) 171–182.

[57] L. Galluzzi, I. Vitale, J.M. Abrams, E.S. Alnemri, E.H. Baehrecke, M. V Blagosklonny, T.M. Dawson, V.L. Dawson, W.S. El-Deiry, S. Fulda, Molecular definitions of cell death subroutines: recommendations of the Nomenclature Committee on Cell Death 2012, Cell Death Differ. (2011).

[58] R. Scherz-Shouval, E. Shvets, E. Fass, H. Shorer, L. Gil, Z. Elazar, Reactive oxygen species are essential for autophagy and specifically regulate the activity of Atg4, Embo J. 26 (2007) 1749–1760.

[59] G. Harris, T. Palosaari, Z. Magdolenova, M. Mennecozzi, J.M. Gineste, L. Saavedra, A. Milcamps, A. Huk, A.R. Collins, M. Dusinska, M. Whelan, Iron oxide nanoparticle toxicity

testing using high-throughput analysis and high-content imaging., Nanotoxicology. 9 Suppl 1 (2015) 87–94.

[60] S. Hackenberg, A. Scherzed, A. Gohla, A. Technau, K. Froelich, C. Ginzkey, C. Koehler, M. Burghartz, R. Hagen, N. Kleinsasser, Nanoparticle-induced photocatalytic head and neck squamous cell carcinoma cell death is associated with autophagy, Nanomedicine. 20 (2013) 1–13.

[61] D.N. Johnson-Lyles, K. Peifley, S. Lockett, B.W. Neun, M. Hansen, J. Clogston, S.T. Stern, S.E. McNeil, Fullerenol cytotoxicity in kidney cells is associated with cytoskeleton disruption, autophagic vacuole accumulation, and mitochondrial dysfunction, Toxicol. Appl. Pharmacol. 248 (2010) 249–258.

[62] F. Wang, M.G. Bexiga, S. Anguissola, P. Boya, J.C. Simpson, A. Salvati, K. a Dawson, Time resolved study of cell death mechanisms induced by amine-modified polystyrene nanoparticles., Nanoscale. 5 (2013) 10868–76.

[63] L. Chen, B. Zhang, M. Toborek, Autophagy Is Involved In Nanoalumina-Induced Cerebrovascular Toxicity, Nanomedicine Nanotechnology, Biol. Med. (2012).

[64] B.H. Kenzaoui, C.C. Bernasconi, S. Guney-Ayra, L. Juillerat-Jeanneret, Induction of oxidative stress, lysosome activation and autophagy by nanoparticles in human brain-derived endothelial cells, Biochem. J. 441 (2012) 813–821.

[65] R.A. Sperling, W.J. Parak, Surface modification, functionalization and bioconjugation of colloidal inorganic nanoparticles, Philos. Trans. R. Soc. A Math. Phys. Eng. Sci. 368 (2010) 1333–1383.

[66] B. Pelaz, P. del Pino, P. Maffre, R. Hartmann, M. Gallego, S. Rivera-Fernández, J.M. de la Fuente, G.U. Nienhaus, W.J. Parak, Surface Functionalization of Nanoparticles with Polyethylene Glycol: Effects on Protein Adsorption and Cellular Uptake, ACS Nano. 9 (2015) 6996–7008.

[67] S.J. Soenen, B.B. Manshian, A.M. Abdelmonem, J.M. Montenegro, S. Tan, L. Balcaen, F. Vanhaecke, A.R. Brisson, W.J. Parak, S.C. De Smedt, K. Braeckmans, The cellular interactions of PEGylated gold nanoparticles: Effect of PEGylation on cellular uptake and cytotoxicity, Part. Part. Syst. Charact. 31 (2014) 794–800.

[68] A. Nagy, A. Zane, S.L. Cole, M. Severance, P.K. Dutta, W.J. Waldman, Contrast of the Biological Activity of Negatively and Positively Charged Microwave Synthesized CdSe/ZnS Quantum Dots, Chem. Res. Toxicol. 24 (2011) 2176–2188.

[69] L.W. Zhang, N.A. Monteiro-Riviere, Mechanisms of quantum dot nanoparticle cellular uptake., Toxicol. Sci. 110 (2009) 138–55.

[70] J. Lovrić, H.S. Bazzi, Y. Cuie, G.R.A. Fortin, F.M. Winnik, D. Maysinger, Differences in subcellular distribution and toxicity of green and red emitting CdTe quantum dots., J. Mol. Med. (Berl). 83 (2005) 377–85.

[71] S.T. Stern, P.P. Adiseshaiah, R.M. Crist, Autophagy and lysosomal dysfunction as emerging mechanisms of nanomaterial toxicity, Part. Fibre Toxicol. 9 (2012).

[72] D. De Stefano, R. Carnuccio, M.C. Maiuri, Nanomaterials Toxicity and Cell Death Modalities, J. Drug Deliv. 2012 (2012).

[73] C. Settembre, A. Fraldi, L. Jahreiss, C. Spampanato, C. Venturi, D. Medina, R. de Pablo, C. Tacchetti, D.C. Rubinsztein, A. Ballabio, A block of autophagy in lysosomal storage disorders., Hum. Mol. Genet. 17 (2008) 119–29.

[74] D. Huang, H. Zhou, J. Gao, Nanoparticles modulate autophagic effect in a dispersity-dependent manner, Sci. Rep. 5 (2015) 14361.

[75] M.N. Moore, Autophagy as a second level protective process in conferring resistance to environmentally-induced oxidative stress, Autophagy. 4 (2008) 254–256.

[76] S.A. Jones, K.H.G. Mills, J. Harris, Autophagy and inflammatory diseases., Immunol. Cell Biol. 91 (2013) 250–8.

[77] https://clinicaltrials.gov/, (n.d.).

[78] X. Michalet, F.F. Pinaud, L.A. Bentolila, J.M. Tsay, S. Doose, J.J. Li, G. Sundaresan, A.M. Wu, S.S. Gambhir, S. Weiss, Quantum dots for live cells, in vivo imaging, and diagnostics., Science. 307 (2005) 538–44.

[79] N. Mizushima, M. Komatsu, Autophagy: renovation of cells and tissues., Cell. 147 (2011) 728–41.

[80] C. Slattery, A. Lee, Y. Zhang, D.J. Kelly, P. Thorn, D.J. Nikolic-Paterson, G.H. Tesch, P. Poronnik, In vivo visualization of albumin degradation in the proximal tubule., Kidney Int. 74 (2008) 1480–6.

10. Figure captions

Figure 1. Schematic design of a core-shell QD (A) and a gradient alloyed QD (B). A core-shell QD commonly exists of a metal core enveloped by an inorganic shell and a coating that renders them water-soluble and allows for further conjugation.[78] In case of gradient alloyed QDs, the defined core-shell interface within the QD is replaced by a gradient composition.

Figure 2. Overview of the mechanistic steps of autophagy and cellular markers investigated in this study.

Autophagy initiates with the synthesis of a phagophore that, while sequestering cytoplasmic cargo, elongates and closes to form a double-membraned autophagosome. During the creation of this autophagosome cytoplasmic LC3-I is activated by lipidation, forming LC3-II, and incorporated into the autophagosomal membrane. The specific targeting of cytoplasmic components for degradation is mediated by p62, a protein that links LC3 with the respective materials. Next, the autophagosome fuses with a lysosome that supplies the acidic pH and enzymes for degradation of the cargo carried by the autophagosome. In the resulting vesicle, the auto(phago)lysosome, the cargo is degraded after which the resulting macromolecules are transported into the cytoplasm by permeases. Since during this step also the inner membrane of the autolysosome is degraded, the LC3-II within the

vesicle is lysed; the LC3-II on the outside is recycled back to LC3-I. The overall process, from autophagosome maturation to its degradation is often referred to as autophagy flux.[79] Since the buffer chloroquine (CLQ) leads to lysosomal alkalinization we applied it throughout our study to mimick lysosomal impairment. Considering this lysosomal impairment causes a block in autophagosome-lysosome fusion further down the line, we also used CLQ as a positive control for increased autophagosomal abundance due to reduced autophagosomal degradation.[44] As lysosomal markers we made use of: LAMP-1, a membrane protein selective for lysosomes;[41] LysoTracker, a dye that primarily accumulates in lysosomes; and DQ BSA, a dye that is selectively degraded by the lysosomal pathway seeing it enters the cell via endocytosis.[80]

Figure 3. Quantum dot characterization Size (A) and zeta-potential (B) of the QDs in HEPES and PBS. Error bars represent the SEM.

Figure 4. Uptake of QDs in HeLa cells. Uptake was determined by flow cytometry after 24h of QD exposure in full medium (n=3). The x-axis denotes the QD dosage: for PEGylated QDs this ranges from 20 to 100nM, while for MPA-coated QDs this ranges from 80 to 200nM. PEGylated QDs are easily taken up at low concentrations though uptake reaches a maximum around 40 nM. MPA-coated QDs are taken up proportionally with increasing dosage, though are only taken up efficiently at higher concentrations. 20 nM of PEGylated QDs leads to similar intracellular fluorescence levels as 125 nM of MPA-coated QDs. Similarly, incubation with 50 nM of PEGylated QDs results in similar intracellular fluorescence levels as 175 nM of MPA-coated QDs. Error bars represent the SEM.

Figure 5. Quantum dot induced acute toxicity and oxidative stress. PEGylated QDs induce cytotoxicity and oxidative stress, MPA-coated QDs are non-toxic up to 200 nM and reduce oxidative stress. (**A**) relative viability compared to untreated cells (100%) determined by the MTT assay (n=6). (**B**) relative level of CellROX intensity compared to untreated cells (100%) determined by flow cytometry (n=6). Error bars represent the SEM.

Figure 6. Impact of Quantum Dots on lysosomal health. PEGylated QDs induce lysosomal impairment, while MPA-coated cause lysosomal activation. (A) relative level of LysoTracker intensity compared to untreated cells (100%) determined by flow cytometry (n=4). (B) Confocal microscopy on LAMP-1 immunostained cells after 24h of exposure to 50 nM PEGylated QDs, 175 nM of MPA-coated QDs or 4 h of 50 µM chloroquine (CLQ). N indicates the nucleus, arrows indicate swollen lysosomes. Scale bar: 20µm. (C) relative level of DQ BSA intensity compared to untreated cells (100%) determined by flow cytometry (n=4). Error bars represent the SEM.

Figure 7. Impact of Quantum Dots on autophagy. PEGylated QDs induce autophagy dysfunction, MPA-coated QDs do not influence autophagic markers. (A) relative level of GFP-LC3 intensity compared to untreated cells (100%) determined by flow cytometry (n=6). Error bars represent the SEM. (B) Confocal microscopy on LC3-immunostained cells after 24h incubation of 50 nM PEGylated

QDs, 175 nM of MPA-coated QDs or 4 h of 50 µM chloroquine (CLQ). N indicates the nucleus, arrows indicate large autophagosomes. Scale bars: 20µm (C) Western blot on autophagic markers LC3 and p62.

Figure 8. Overview of the distinct cellular effects of GA QDs coated with PEG or MPA.

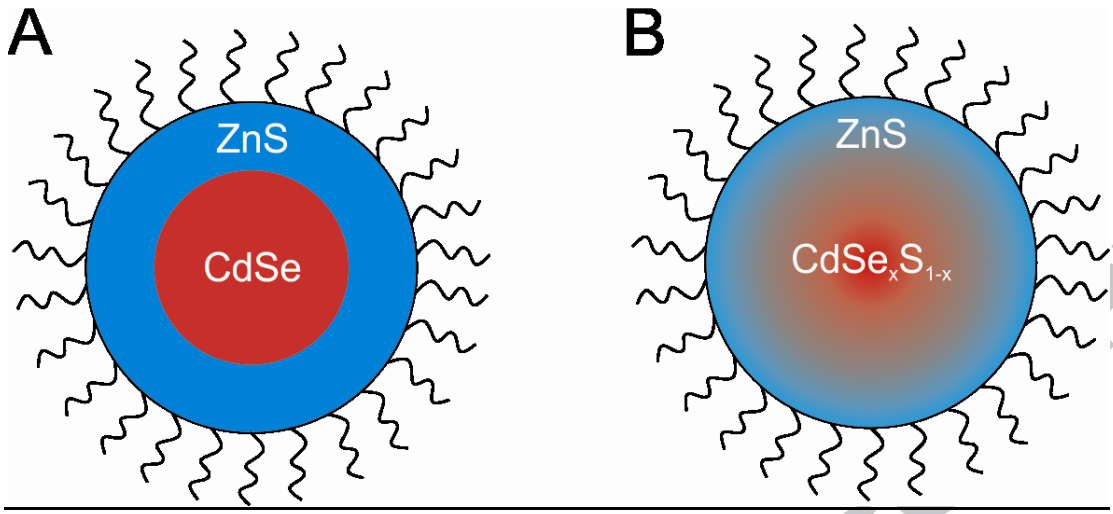

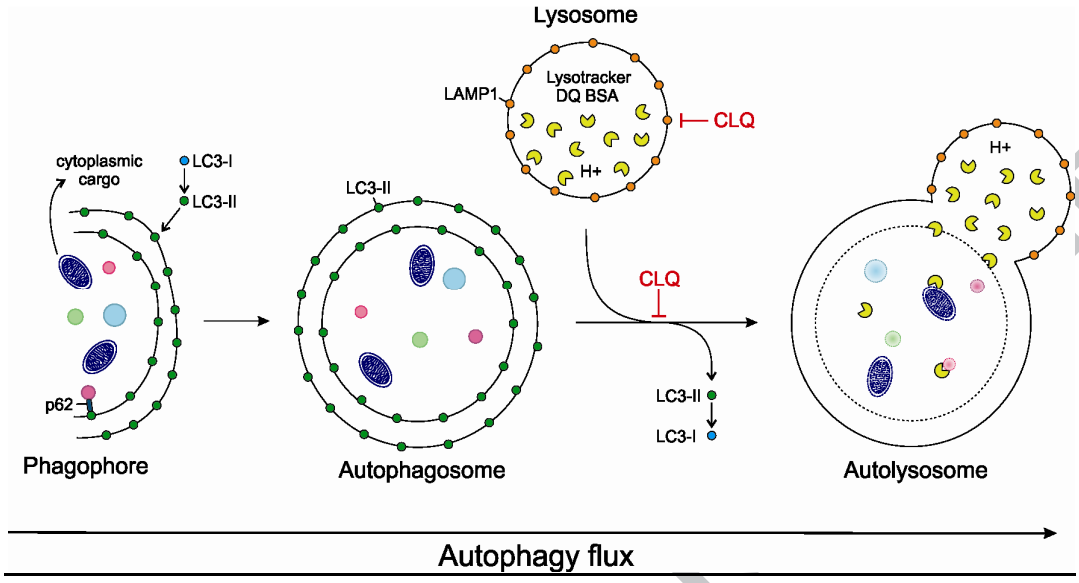

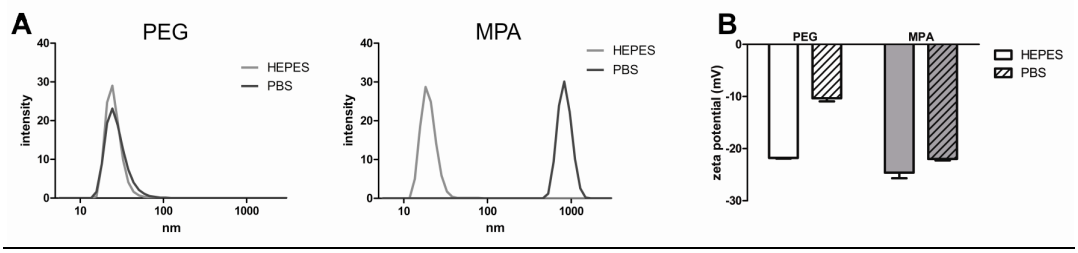

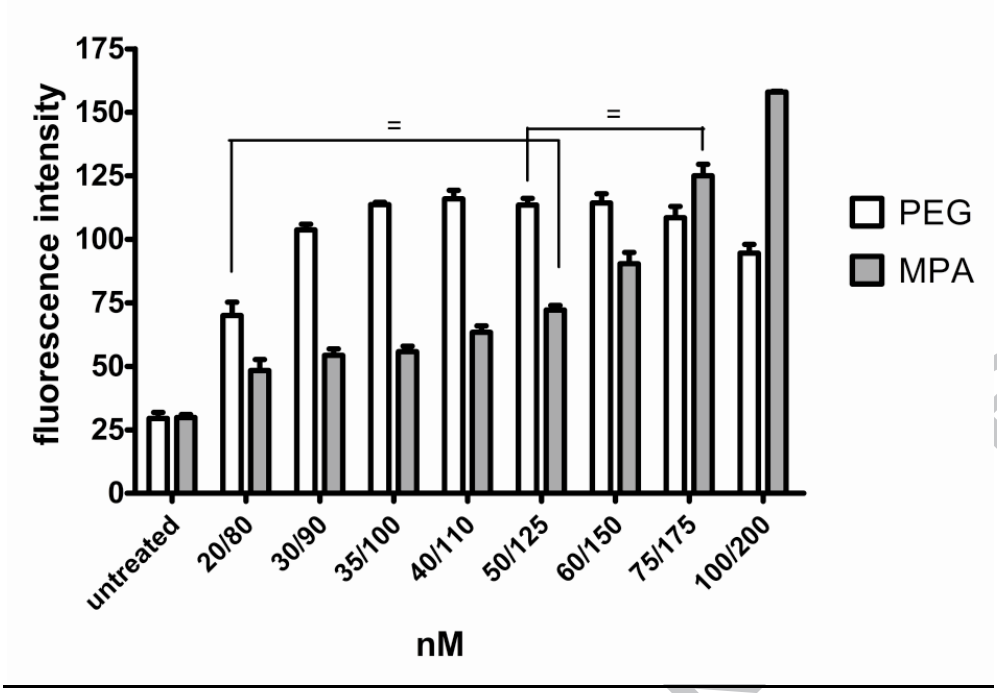

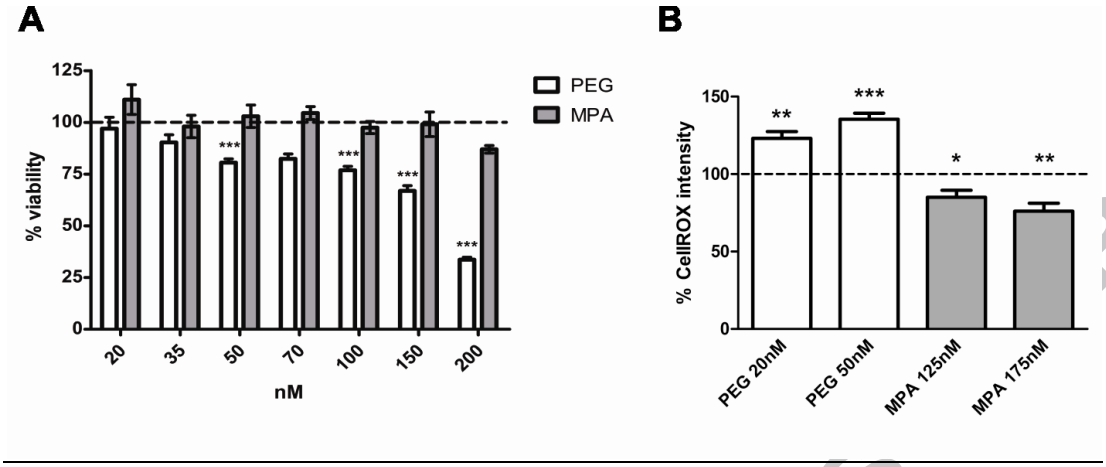

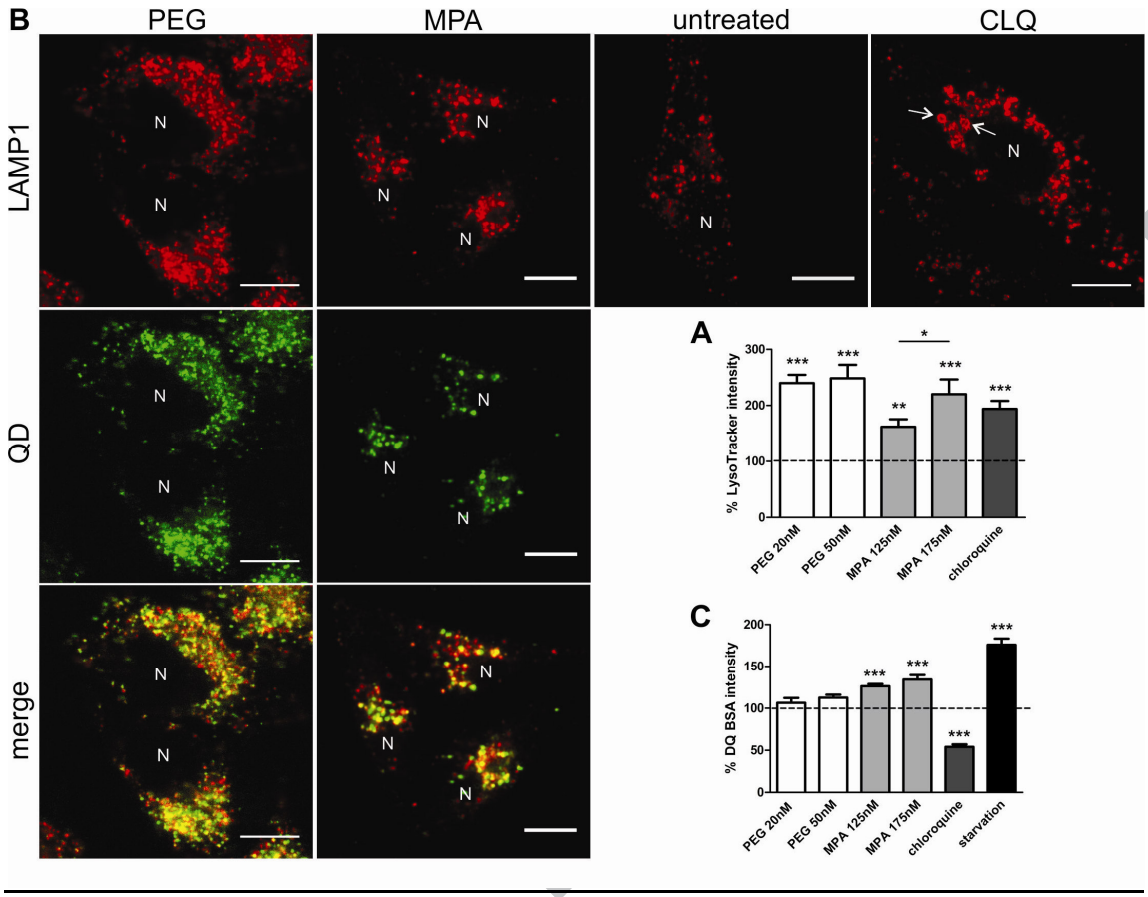

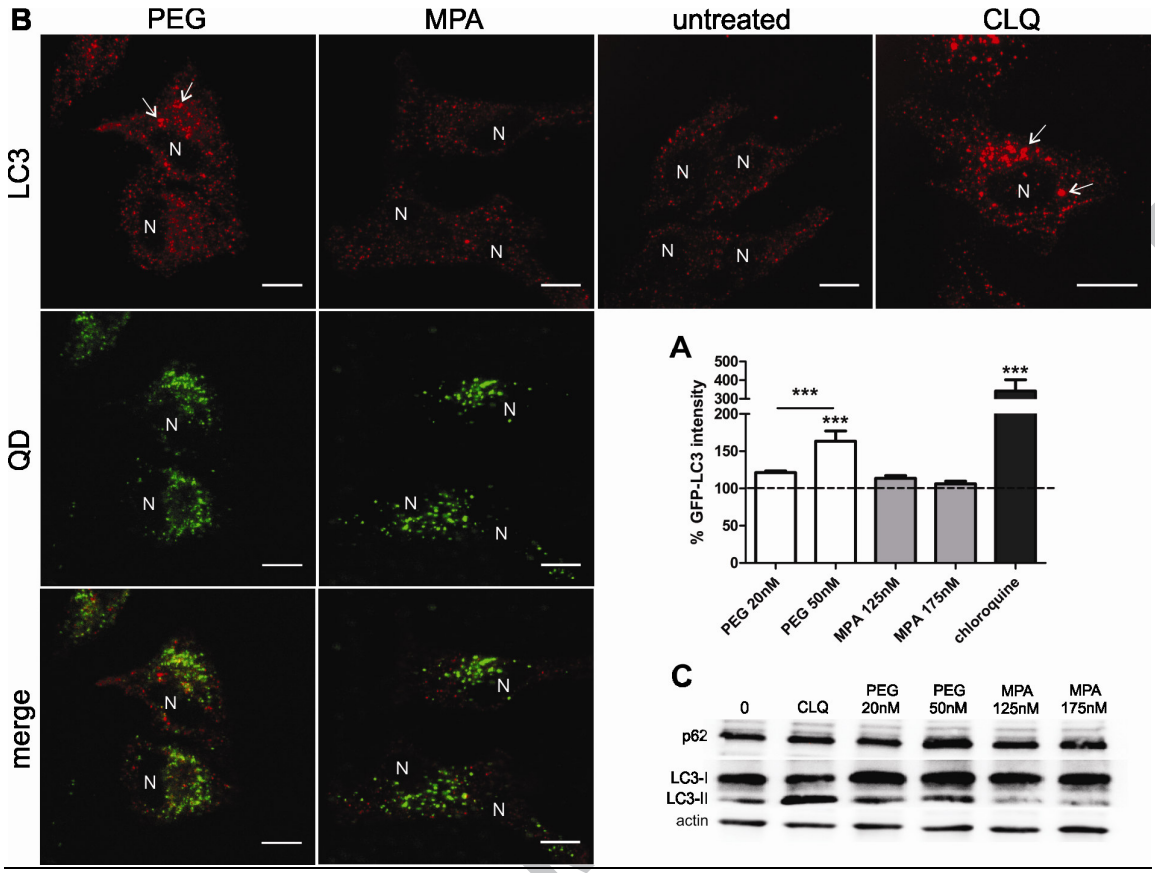

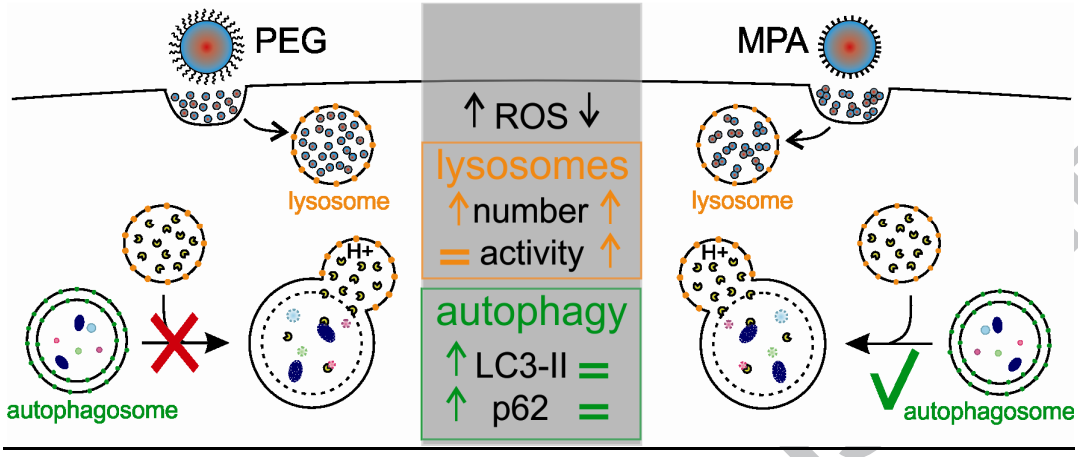

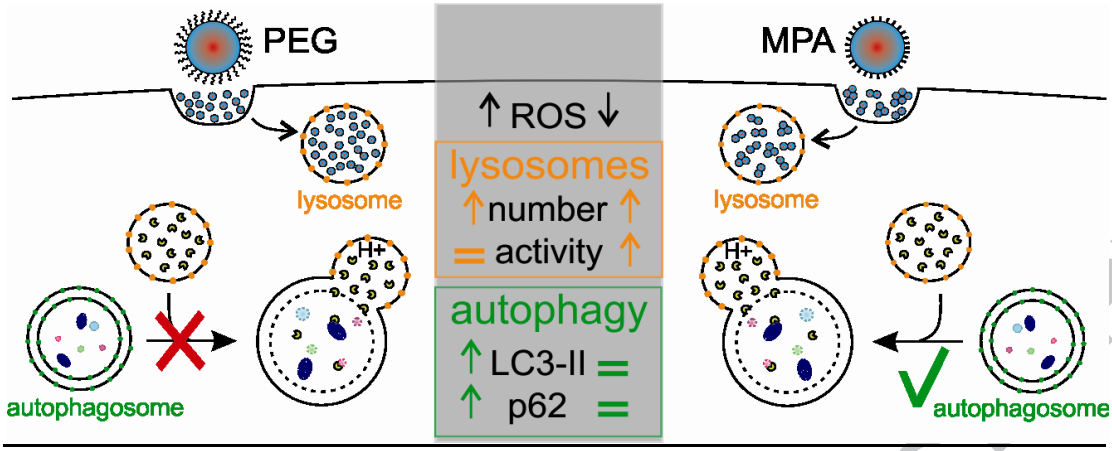

Statement of Significance

Gradient alloyed Quantum Dots (GA-QDs) are highly promising nanomaterials for biomedical imaging seeing they exhibit supremely fluorescent properties over conventional QDs. The translation of these novel QDs to the clinic requires a detailed toxicological examination, though the data on this is very limited. We therefore applied a systematic approach to examine the toxicity of GA-QDs coated with two commonly applied surface ligands, this while focusing on the autophagy pathway. The impact of QDs on this pathway is of importance since it has been connected with various diseases, including cancer. Our data accentuates that the coating defines the impact on autophagy and therefore the toxicity induced by QDs on cells: while MPA coated QDs were highly biocompatible, PEGylated QDs were toxic.